The influence of phenolic acyl groups on the color of purple sweet potato anthocyanins and their metal complexes

Julie-Anne Fenger, Hugo Roux, Rebecca Robbins, Thomas Collins, Olivier O. Dangles

The influence of phenolic acyl groups on the color of purple sweet potato anthocyanins and their metal complexes

Julie-Anne Fenger,[a*] Hugo Roux,[a] Rebecca J. Robbins,[b] Thomas M. Collins,[c] Olivier Dangles[a]*

[a] *Avignon University, INRAE, UMR408, 84000 Avignon, France*
[b] *Mars Wrigley, 1132 W Blackhawk Street, Chicago, IL 60642, USA*
[c] *Retired*

*Corresponding authors.

E-mail addresses: fengerja@gmail.com, olivier.dangles@univ-avignon.fr

Abstract

Anthocyanins from purple sweet potato (PSP) are peonidin and cyanidin glycosides acylated by *p*-hydroxycinnamic and *p*-hydroxybenzoic acids. For six individual PSP pigments, the thermodynamic constants of proton transfer and water addition were determined, from which the speciation diagrams for the colored and colorless forms and the UV-visible spectra of individual colored forms could be constructed. The data confirm that acylation by phenolic acids protects the chromophore against water addition (a consequence of acyl – anthocyanidin π-stacking interactions) and that this protection depends on the type and number of acyl residues, diacylation being much more efficient than monoacylation, and *p*-hydroxycinnamoyl more efficient than *p*-hydroxybenzoyl. Most PSP anthocyanins can bind metal ions (Fe^{2+}, Al^{3+}) through their cyanidin chromophore and/or their caffeoyl residue(s). At pH 7, a cyanidin glycoside bearing a caffeoyl residue can bind a single metal ion by simultaneous involvement of its two binding units. With Fe^{2+} a strong bluing effect was observed. Although the caffeoyl residues efficiently slow down color loss, their redox activity actually accelerates the thermal degradation of anthocyanins. Consistently, two-electron autoxidation of anthocyanins bearing caffeoyl residues could be evidenced by UPLC-MS/DAD analysis. These new pigments possibly stem from intramolecular coupling between the chromophore and *o*-quinones derived from the caffeoyl residues.

1. Introduction

Anthocyanins are plant pigments that typically exhibit bright red, purple and blue colors as the pH is changed from 1 to 9 [1,2]. This property makes them potential natural food colorants. However, color instability in the pH range 4 - 7 greatly limits the industrial applications of anthocyanins. Color loss results from a combination of reversible (water addition) and irreversible (autoxidation, hydrolysis) mechanisms [3]. Polyacylation by phenolic acids, *i.e*. hydroxycinnamic acids (HCAs) or hydroxybenzoic acids (HBAs), efficiently increases the color stability owing to π-stacking interactions between the anthocyanidin chromophore and the acyl residues. Within the compact conformations (intramolecular copigmentation) and/or aggregates (self-association) thus formed, the anthocyanidin is less available to attacks by bleaching agents, such as water, bisulfite and hydrogen peroxide [4]. Polyacylated anthocyanins, which are common in flower petals, can also be found in edible sources, especially in intensely colored vegetables, such as red cabbage (RC) and purple sweet potato (PSP), and the corresponding extracts bear great potential for application as food colorants.

RC and PSP anthocyanins are both 3-O-sophorosyl-5-O-glucosylcyanidin and peonidin derivatives bearing a variety of acyl groups on the sophorosyl moiety. In RC, acylation occurs at C6-OH of the first D-glucose unit (Glc-1) and/or at C2-OH of the second D-glucose unit (Glc-2). By contrast, acylation in PSP anthocyanins only occurs at the C6-OH positions of both Glc units (Scheme 1). Diacylation of RC and PSP anthocyanins provides a remarkable protection against water addition to the C2 position (C-ring) of the flavylium ion (AH^+), which leads to a colorless hemiketal (B) in equilibrium with minor concentrations of *cis*- and *trans*-chalcones (Cc and Ct) (Scheme 1-SI) [5,6]. Sandwich-type conformations with the chromophore intercalated between the two acyl residues are assumed to be involved in this gain in color stability [7].

While PSP anthocyanins are most commonly peonidin (major) and cyanidin (minor) derivatives, RC are essentially cyanidin derivatives, which were shown to bind metal ions above pH 5 with concomitant intense bathochromic shifts in the visible band and color stabilization [8]. Unlike their RC cabbage homologs, some major PSP pigments have a caffeic acid residue, which itself can bind metal ions. Hence, depending on the PSP anthocyanin selected, metal binding can occur via the chromophore (RC anthocyanins) or acyl group (P9a, P10, P11, P12) or both (P9b) (Scheme 1).

In this work, from a selection of individual PSP anthocyanins differing by the number and type (HCA *vs*. HBA) of acyl residues, the influence of acylation on the color loss by reversible water addition was quantitatively investigated. The superiority of anthocyanins bearing two HCA residues is clearly demonstrated. The relative affinity of the cyanidin and caffeoyl binding sites for metal ions and its consequences on the color expressed was investigated at pH 7 with Fe^{2+} and Al^{3+}. Finally, the impact of the caffeoyl residues, free or coordinated to iron, on the irreversible color loss (autoxidation) was also assessed. Evidence for the formation of new pigments derived from intramolecular caffeoyl – anthocyanidin oxidative coupling is provided.

2. Materials and methods

2.1. Chemicals

Anthocyanin extracts and isolated anthocyanins from purple sweet potato and red cabbage (Scheme 1) were isolated by semi-preparative reverse phase HPLC [9]. They are acylated derivatives of cyanidin- or peonidin-3-O-sophorosyl-5-O-glucoside. HPLC-grade water was used for all aqueous solutions. Caffeic acid, $FeSO_4$ - $7H_2O$, $AlCl_3$ - $6H_2O$, KCl, $NaH_2PO_4 \cdot 2H_2O$ and $Na_2HPO_4 \cdot 7H_2O$ were all purchased from Sigma-Aldrich. Acetic acid (VWR), trace metal grade HCl (Fisher Scientific) and NaOH (Alpha Aesar) were also used. Concentrated stock solutions (5 mM) of pigment were prepared in 0.05 M HCl.

2.2. Structural transformations of anthocyanins

For six major PSP anthocyanins, the following parameters were determined according to a method recently described with details [5]: the first and second acidity constants of the flavylium ion pK_{a1} and pK_{a2} (successively connecting the AH^+ and the neutral and anionic bases A and A^-), the overall acidity constant of the flavylium ion pK'_a (defined as $K'_a = K'_h + K_{a1}$), the apparent hydration constant of the flavylium ion pK'_h (connecting AH^+ and the set of hydrated colorless forms, B, Cc and Ct) and the corresponding rate constants of hydration k_h (s^{-1}) and dehydration k_{-h} (M^{-1} s^{-1}). The latter is actually an apparent rate constant for the dehydration of B and Cc in fast tautomeric equilibrium (Scheme 1-SI).

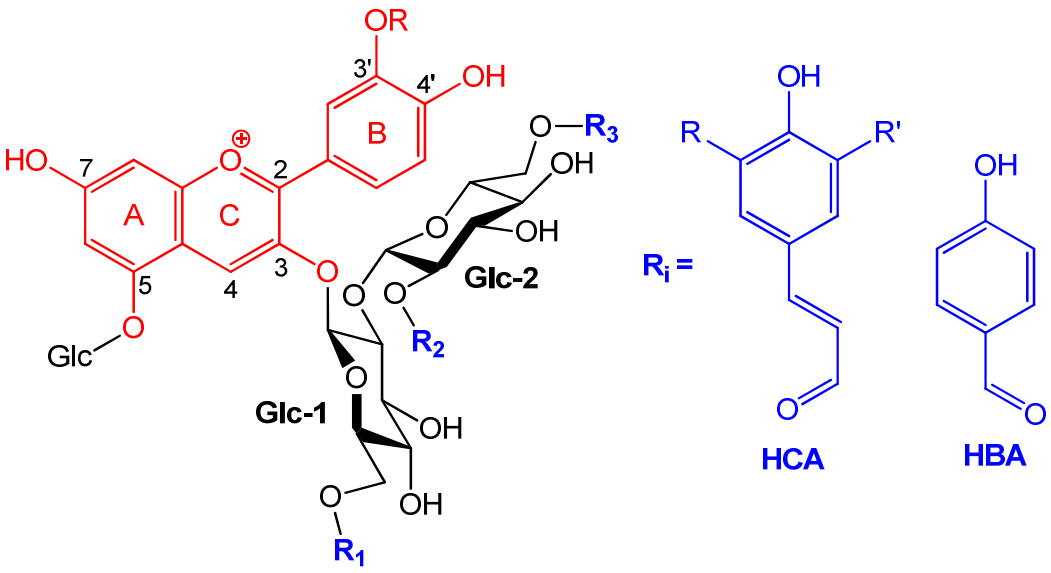

	R	R_1	R_2	R_3
PA'	Me	H	H	H
P9a [a]	Me	Caffeoyl	H	H
P9b [b]	H	Caffeoyl	H	Feruloyl
P10 [b]	Me	Caffeoyl	H	Caffeoyl
P11 [b]	Me	Caffeoyl	H	*p*-Hydroxybenzoyl
P12 [b]	Me	Caffeoyl	H	Feruloyl
PA [c]	H	H	H	H
P4 [c]	H	*p*-Coumaroyl	Sinapoyl	H

p-Coumaroyl (pC): R = R' = H

Caffeoyl (Cf): R = OH, R' = H

Feruloyl (Fl): R = OMe, R = H

Sinapoyl (Sp): R = R' = OMe

[a] Structure inferred from those of the PSP diacylated pigments. [b] Structures from [10].

[c] From red cabbage [5].

Scheme 1. Structure of the purple sweet potato anthocyanins studied

Briefly, 10^{-2} M acetate (pH 3.0 – 6.0) and phosphate (pH 6.0 – 8.5) buffers were used and the ionic strength fixed with 0.1 M KCl. Absorption spectra were recorded on a Agilent 8453 diode-array spectrometer in thermostated and magnetically stirred quartz cuvettes (pathlength = 1 cm). For each pigment, the kinetics of the hydration reaction was monitored over the pH range 2 - 6. The apparent first-order rate constant of hydration (k_{obs}) was calculated for each final pH value. The first acidity constant K_{a1} (AH^+/A couple) and rate constants k_h and k_{-h} were deduced from the pH dependence of k_{obs} and the ratio of the initial to final visible absorbance [5]. These solutions were left for 1 - 2 h to reach the hydration

equilibrium and their UV-visible spectra were recorded. From the plot of A_{eq} (at the flavylium's λ_{max}) as a function of pH in the range 1 - 6, the apparent acidity constant pK'_a was estimated (example provided in Fig. 1-SI). The apparent hydration constant K'_h was deduced from the relationship: $K'_a = K'_h + K_{a1}$. Finally, the second acidity constant K_{a2} (A/A$^-$ couple) was estimated from the pH dependence of the absorbance at the anionic base's λ_{max} immediately after addition of pigment to near neutral solutions (pH 6.0 - 8.5). Under such conditions, the slow hydration can be neglected. By expanding the pH range to 9.2 and by monitoring in the UV range (375 nm), the first acidity constant of P9a's caffeoyl moiety could also be estimated.

Speciation diagrams showing the pH-dependence of the individual forms were constructed from the pK_{a1}, pK_{a2} and pK'_a values (Fig. 2-SI). They were determined at $t = 0$ (hydration excluded) and at equilibrium.

2.3. Colorimetric data

In the color industry, it is common to express color characteristics by the L*a*b* coordinates. L* corresponds to the light intensity, expressed from 0 (no light) to 100. Parameters a* and b* quantify the contribution of four colors: green (-a), red (+a), blue (-b) and yellow (+b). A program was developed that converts the UV-visible spectra (from 380 to 780 nm with 5 nm intervals) to the XYZ tri-stimulus values, then to the L*a*b* coordinates, using the CIE (Commission Internationale de l'Eclairage) equations [11] for the standard D_{65} illuminant and an observer at 10° (see Table 1-SI). From these coordinates, an open-access online digital color calculator (http://colorizer.org/) was used to create color patches that provide a reliable picture of the color actually expressed by the pigments in solution at a concentration of 50 µM.

2.4. Metal binding experiments

Fresh 5 mM solutions of Fe^{2+} and Al^{3+} were prepared from $FeSO_4$ - $7H_2O$ and $AlCl_3$ - $6H_2O$ in 1 mM HCl. In the quartz cuvette of the UV-visible spectrometer, the following solutions were added in this order: pH 7 phosphate buffer, 20 µL of anthocyanin stock solution and, after a few seconds, a small volume of the 5 mM Fe^{2+} solution (final iron/anthocyanin molar ratio = 1 or 2). The full UV-visible spectra were recorded in kinetic mode. The duration of acquisition varied between 1 and 2 min. For an optimal sensitivity, the detection in the visible range was set at 550 or 610 nm with Al^{3+} (close to the complex's λ_{max}) and at 670 nm with Fe^{2+} (charge transfer contribution of the Fe^{3+} complexes). For free and

bound caffeic acid, the absorbance was recorded at 350 nm and 370 nm, respectively. When applicable, the hyperchromic and bathochromic shifts were calculated from the initial (free ligand) and final (metal complex) spectra as $(A_{max,f} - A_{max,0})/A_{max,0}$ and $\lambda_{max,f} - \lambda_{max,0}$, respectively.

2.5. Kinetic modeling

The kinetic curves were analyzed with the Scientist® software (Micromath, St Louis, USA). A two-step process was usually observed, which is interpreted as the successive formation of complex C1 (second-order rate constant k_1, molar absorption coefficient ε_1) evolving into complex C2 (first-order rate constant k_2, molar absorption coefficient ε_2). Optimized values for the rate constants and molar absorption coefficients are reported.

2.6. Thermal degradation

Thermal degradation was performed at pH 7 and 50°C in a thermostated water bath according to a method previously reported [4]. Briefly, the pigments were diluted to 50 µM in the phosphate buffer at 50°C and UV-vis spectra were recorded over 8h. The residual fraction of color species at pH 7 (a mixture of neutral and anionic bases) was determined at λ_{max} as % Color = 100 x $A_{\lambda max}(t)$ / $A_{\lambda max}(t = 0)$. Aliquots of 1.5 mL were taken up at time zero, at regular time intervals over 8h, and finally at t = 24 and 48h. They were cooled down, acidified to pH 1 and stabilized at room temperature for 15h (nonacylated anthocyanins) to 48h (diacylated anthocyanins) (to ensure complete regeneration of the flavylium ion from the colorless forms). The absorption spectra were then recorded and the residual fraction of flavylium ion was calculated as % AH^+ = 100 x $A_{\lambda max}(t)$ / $A_{\lambda max}(t = 0)$ and plotted as a function of time. Finally, the percentage of degradation products was simply deduced from % D = 100 – % AH^+.

2.7. Product identification

The acidified and stabilized samples were analyzed with an Acquity UPLC (Waters Corporation, Milford, USA) equipped with a diode array detector (DAD) and a ESI-Q-trap HCT Ultra mass spectrometer (Bruker Daltonics, Bremen, Germany) in ultrascan mode. Samples (5 µL) were injected onto an Acquity UPLC BEH C18 reversed phase column (50x2.1 mm, 1.7 µm) at 30°C. Phase A (1% HCO_2H in H_2O) and B (1% HCO_2H in MeCN) were used for elution at 0.4 mL/min. Gradient for P12 was %B: 0 min: 6%, 3 min: 12%, 9 min: 18%, 11 min: 24%, 14 min: 80%, 15-18 min: 6%. Gradient for P4 was %B: 0 min: 6%, 5 min: 12%, 10 min: 24%, 12-13 min: 80%, 15-18 min: 6%. The capillary voltage was -1.8 kV

(positive mode) or 2.2 kV (negative mode) with a 120-2200 *m/z* scanning interval at a speed of $26x10^3$ *m/z* s^{-1}. Desolvation was conducted with N_2 at 365°C, 40 psi, 540 L/h. The cone voltage and the fragmentation amplitude were 40 V and 1.2 V, respectively.

3. Results and discussion

3.1. Structural transformations of PSP anthocyanins

Non-, mono- and diacylated anthocyanins were compared through the thermodynamic and kinetic parameters characteristic of their structural transformations in acidic to mildly alkaline solution (Scheme 1-SI). Whereas the first and second acidity constants are weakly impacted by the acylation with no clear trend emerging, the overall acidity constant, which includes the hydration component, is strongly affected: the pK'_a value increases from nonacylated to diacylated anthocyanins, with a gap more marked when a second acyl residue is introduced. As expected, this trend is translated in the pK'_h value, the global thermodynamic constant of water addition to the flavylium ion. The diacylated anthocyanins of purple sweet potato appear much more resistant to water addition than their non- and monoacylated analogs, meaning that the second acyl residue triggers a better protection of the flavylium ion against water addition than the first one, as observed with the red cabbage anthocyanins [5]. This is consistent with the hypothesis of diacylated anthocyanins adopting sandwich conformations with the anthocyanidin intercalated between the 2 acyl residues for optimal protection. The second acylation also occurs on the external sugar of the sophorose, and thus displays a higher flexibility. This may result in more efficient π-stacking interactions.

The speciation diagrams express the calculated fractions of flavylium, neutral base, anionic base and the mixture of colorless forms, plotted for each pigment over the pH range 1 – 10. They show that the fraction of colored forms in mildly acidic solution (pH 5 - 7) ranges from *ca*. 1% for PA' to *ca*. 60% for P9b. As for the red cabbage anthocyanins [5], the coloring potential of the diacylated anthocyanins far outreaches that of the non- and monoacylated homologs at all pHs. This protection against hydration is mostly rooted in smaller hydration rate constants (a factor *ca*. 30 between the k_h values of PA' and P12). As diacylated anthocyanins make a large contribution to PSP anthocyanin extracts, representing

48% to 75% or more according to the cultivar [12,13], these pigments are mostly responsible for the color of the extract at the typical food pHs.

Table 1. Thermodynamic and rate constants for the structural transformations of the PSP anthocyanins (25°C).

	Pigment	pK'_a	pK_{a1}	pK_{a2}	pK'_h [a]	pK_h [b]	k_h (s^{-1})	k_{-h} (M^{-1} s^{-1})
PA'	Peo	2.04 (± 0.04)	4.21 (± 0.08)	7.08 (± 0.04)	2.04	2.55	0.33 (± 0.01)	116 (± 7)
P9a	Peo(Cf)	2.43 (± 0.02)	4.06 (± 0.12)	7.11 (± 0.02)	2.44	2.82	0.132 (± 0.011)	87.8 (± 6.6)
P9b	Cya(Cf,Fl)	3.71 (± 0.07)	3.93 (± 0.04)	7.15 (± 0.06)	4.11	3.91	0.049 (± 0.004)	394 (± 24)
P10	Peo(Cf,Cf)	3.53 (± 0.03)	4.11 (± 0.06)	7.16 (± 0.05)	3.66	3.95	0.028 (± 0.004)	251 (± 25)
P11	Peo(Cf,HB)	3.25 (± 0.03) [c]	3.99 (± 0.06) [c]	7.29 (± 0.02) [c]	3.34	3.74	0.030 (± 0.004)	162 (± 16)
P12	Peo(Cf,Fl)	3.85 (± 0.04)	4.34 (± 0.07)	7.49 (± 0.05)	4.02	4.25	0.010 (± 0.002)	176 (± 27)

[a] $K'_h = K'_a - K_{a1}$ (Ct included), [b] $K_h = k_h / k_{-h}$ (Ct excluded). [c] From [6] (phosphate / citrate / borate buffer): pK'_a = 3.15, pK_{a1} = 4.2, pK_{a2} = 7.8. Peo(HB): pK'_a = 2.69, pK_{a1} = 4.1, pK_{a2} = 7.5.

Among the diacylated anthocyanins of PSP, P11 bears a *p*-hydroxybenzoyl residue, which is much less common than the hydroxycinnamoyl residues. This peculiarity makes P11 more vulnerable to water addition than the other diacylated pigments (P9b, P10 and P12), which display 2 HCA residues. For instance, the percentage of colored forms at equilibrium at pH 7 is *ca*. 40% for P12, *vs*. only 10% for P11. In addition, the formation of the colorless species (hydration) is 3 times as fast with P11 as for P12. This is consistent with HBAs being less potent copigments than HCAs [7] and suggests that the HBA residue of P11 develops

weaker π-stacking interactions with the anthocyanidin than the wider more polarizable HCA residues.

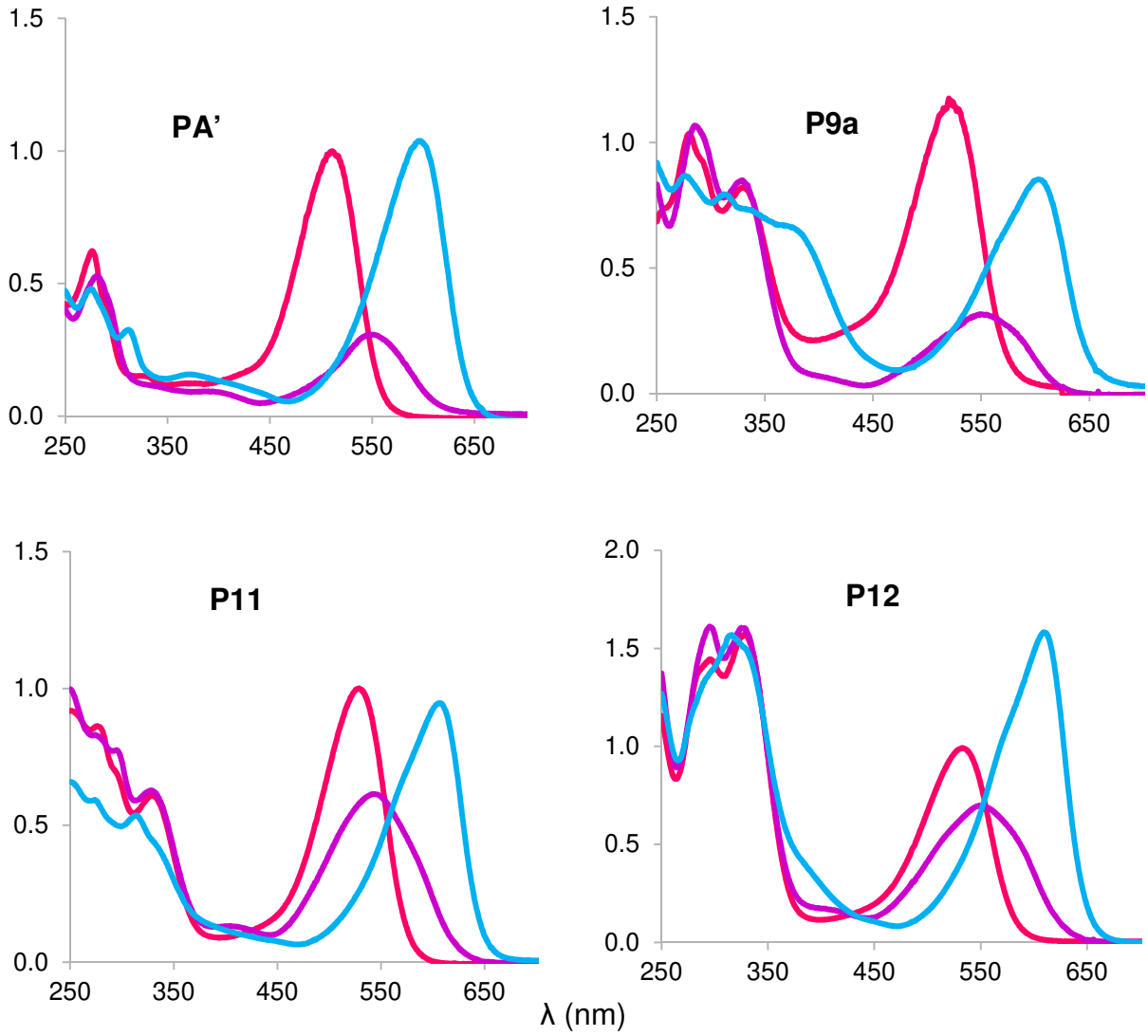

λ_{max} (nm)	Flavylium ion	Neutral base	Anionic base
PA' (no acyl)	511	548	597
P9a (acyl = Cf)	522	542	603
P11 (acyl = Cf, HB)	528	543	607
P12 (acyl = Cf, Fl)	528	553	610

Fig. 1. UV-visible spectra of pure colored forms for peonidin derivatives PA', P9a, P11 and P12. —: flavylium ion, —: neutral base, —: anionic base; color patches (from the L*a*b*coordinates).

The spectra of the pure neutral and anionic bases can be calculated from the experimental spectra at pH 1 (pure flavylium), 5.5 and 7.5 (recorded before significant hydration) and the pK_{a1} and pK_{a2} values. For instance, from the total pigment concentration and the pK_{a1} value, the concentration of the flavylium ion is determined at pH 5.5 and the corresponding spectrum is generated, then subtracted from the experimental one, thus yielding the spectrum of the pure base. This spectrum can then be used for similar corrections at pH 7.5 to unveil the spectrum of the pure anionic base. Such analyses permit to rigorously compare the coloring properties for a selection of peonidin derivatives from PSP as a function of their acylation pattern (Fig. 1). As usual, acylation results in a shifting of the visible band to higher wavelengths but this phenomenon, typically associated with acyl – anthocyanidin π-stacking interactions, is more significant with the flavylium ion and the anionic base. Acylation by a *p*-hydroxybenzoyl *vs*. *p*-hydroxycinnamoyl residue has no consequence on the flavylium spectrum (same λ_{max} for P11 and P12) but results in slightly lower λ_{max} values for the neutral and anionic bases (Fig. 1).

The spectra of the anionic bases of P9a, P9b and P12 all show a narrow asymmetric absorption band associated with a high chromaticity (Table 1-SI), which is an advantage in terms of color expression. Based on our previous work [5], purple sweet potato and red cabbage diacylated anthocyanins (except for P11) cannot be discriminated by their sensitivity to water addition. Thus, the position on Glc-2 of the second HCA residue (C6-OH in PSP *vs*. C2-OH in RC) has little influence on its capacity to hinder water addition to the flavylium ion.

From the spectral changes in the UV range at higher pH, the pK_a of the P9a's caffeoyl residue was estimated at 8.27 ± 0.05. This residue is more acidic than free caffeic acid (pK_a = 8.48) [14], 5-caffeoylquinic acid (pK_{a2} = 8.42) [15] and the caffeoyl moiety of the heavenly blue anthocyanin (pK_{a3} = 9.02) [16]. The dissociation of the HCA residues is thus largely negligible at food pHs.

3.2. Metal binding

In our study of metal – anthocyanin binding, a neutral moderately concentrated (10 mM) phosphate buffer was used to set the pH constant and also simply mimic the competition polyphenols may encounter in natural media with other common oxygenated ligands (organic acids, phosphate and phosphatidyl groups) for metal ions. Aluminum and iron binding is an important mechanism of color variation in plants, especially for the expression of blue colors

in flowers [17]. In PSP anthocyanins, the cyanidin nucleus and/or the caffeoyl residues can bind metal ions owing to their catechol rings. For comparison, nonacylated pigment PA and free caffeic acid were also studied. The spectral modifications of the PSP pigments (Fig. 2, Table 2-SI) are highly dependent on pH, the metal ion, and the presence, number and position of acyl residues.

3.2.1. Aluminum binding

Caffeic acid does not bind to 1 molar equiv. of Al^{3+} at pH 7, whether free or as the single acyl group of peonidin derivative P9a (Glc-1). However, for P10, the presence of the second caffeoyl residue (Glc-2) allows Al^{3+} binding (Fig. 2, Table 2-SI).

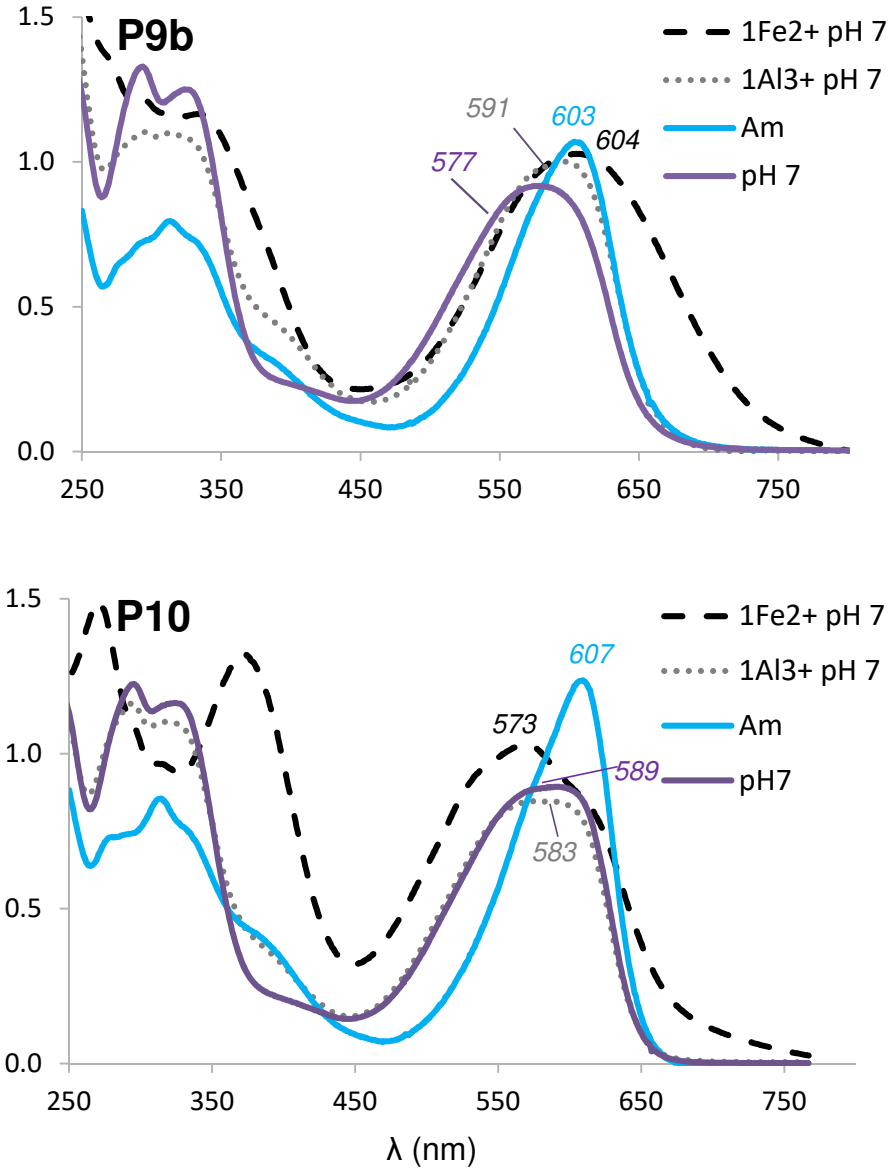

Fig. 2. UV-visible spectra of pigment P9b (Cya, acyl = Cf, HB) and P10 (Peo, acyl = Cf, Cf), at pH 7, its pure anionic base (Am, calculated) and its Fe^{2+} and Al^{3+} complexes (1 equiv.).

The binding of 1 or 2 equiv. Al^{3+} is primarily manifested by weak modifications in the UV band of the acyl residues (the appearance of a shoulder at *ca*. 400 nm), while the visible band remains mostly unaffected. Besides, reaching saturation in the spectral modifications requires an excess Al^{3+}, which suggests that Al^{3+} - P10 binding is reversible under our conditions.

P9b combines two potential binding units, the cyanidin nucleus and the caffeoyl residue on Glc-1 (inert to Al^{3+} as observed with P9a). The spectral changes in the UV range are the same as for P10 but the visible band is now shifted to higher wavelengths and broadened (Fig. 2). Moreover, the final spectra with 1 and 2 equiv. Al^{3+} are almost identical. Overall, these observations suggest a simultaneous binding of 1 equiv. Al^{3+} for the cyanidin and caffeoyl moieties. The absorption spectrum of the P9b - Al^{3+} complex is close to the calculated spectrum of the pure anionic base (Fig. 2). From the anionic base (proton loss from the acidic C7-OH and C4'-OH groups), the coordination of Al^{3+} induces an additional proton loss from C3'-OH, which apparently has only a weak spectral impact.

3.2.2. Iron binding

In a neutral dilute phosphate buffer, natural catechols typically bind Fe^{3+} much more slowly than Fe^{2+} because of the strong competition between phosphate and phenol for Fe^{3+} [18]. However, fast Fe^{2+} binding is typically followed by fast autoxidation of Fe^{2+} within the complexes, which was confirmed by Fe^{2+} titration (ferrozine test). Independent experiments with RC anthocyanins confirmed the much faster binding to Fe^{2+} in a 10^{-2} M phosphate buffer. Moreover, the final spectra were actually the same, whether Fe^{2+} or Fe^{3+} was added, in agreement with iron autoxidation during binding (Fig. 3-SI). Direct high-resolution mass analysis of the solutions also confirmed that the final complexes involve Fe^{3+} (unpublished data). Although free Fe^{2+} is already quite prone to autoxidation in neutral solution, its conversion to Fe^{3+} is expected to be accelerated by binding to catechols, given the much higher intrinsic affinity of these ligands for Fe^{3+} ($\log K_b = 20$ for Fe^{3+}, *vs*. 8 for Fe^{2+} [19]).

Fe^{2+} binding to caffeic acid or P9a results in the formation of a characteristic shoulder (between 350 and 370 nm) from the UV band. By contrast, full deprotonation of caffeic acid (pH *ca*. 10) shifts the absorption band to 344 nm (Fig. 4-SI). With caffeic acid, a new absorption band typical of ligand-to-iron charge transfer is also observed at $\lambda_{max} \approx 610$ nm (Fig. 4-SI) with a weak molar absorption coefficient ($\varepsilon \approx 900$ M^{-1} cm^{-1}). Fe^{3+} being a much stronger electron acceptor than Fe^{2+}, the development of the charge transfer band is another

evidence of Fe^{2+} autoxidation within the complex [18,19]. With P10, the spectral changes in the UV range are much more intense and a true new absorption band at λ_{max} = 374 nm emerges (Fig. 2). Its extension into the visible range adds a yellow component to the P10's color. This new band points to cooperation between the two Cf residues in iron binding. Although the peonidin nucleus has no metal binding ability, iron shifts the visible band to shorter wavelengths (Fig. 2, Table 2-SI). This hypsochromic shift could reflect the perturbation of the peonidin – acyl π-stacking interactions (a consequence of the iron-induced perturbation of the electron density on the caffeoyl residues) and is also another evidence of the compact folded conformations adopted by diacylated anthocyanins.

Caffeic acid - Fe^{2+} binding results in a weak shoulder at 370 nm (Fig. 4-SI), which is not further increased by higher Fe^{2+} concentrations. In the presence of iron, the visible spectrum of PA exhibits a weak bathochromic shift of 9 nm (Fig. 4-SI). Both bindings occur with similar kinetics (Table 2). In comparison with PA and caffeic acid, the spectral modifications induced by Fe^{2+} - P9b binding are much more spectacular (a bathochromic shift of 27 nm and a more intense shoulder at 370 nm) and indicate that both binding sites participate (Figs. 2 & 5-SI).

3.2.3. Binding stoichiometry

In the presence of increasing Fe^{2+} concentrations, the bathochromic shift of P9b's visible band reaches saturation at 1 equivalent (Fig. 6-SI). This is evidence of a dominant 1:1 binding, which is the stoichiometry typically evidenced with other iron – flavonoid complexes [19–21]. However, 1:2 binding was also reported with quercetin and kaempferol [22]. In agreement with a 1:1 iron – anthocyanin binding, the same final UV-visible spectra were recorded with P9b, whether 1 or 2 equiv. Fe^{2+} were added (data not shown). The same observation holds for P10 and Fe^{2+}. By contrast, with caffeic acid, saturation was reached at lower iron concentrations, 1/3 to 2/3 equiv. (Fig. 6-SI), suggesting its possible involvement in 1:2 and 1:3 coordination complexes.

3.2.4. Quantitative kinetic analysis

Simple binding models were used to simultaneously analyze the spectral changes in the visible (anthocyanidin) and UV (acyl) domains (Table 2, Fig. 3).

When metal binding is observed, this is often through a two-step kinetic process (Fig. 3). The 2 kinetic steps can be evidenced at the same monitoring wavelength, either by an

increase in absorbance followed by a decay (*e.g.*, caffeic acid + Fe^{2+}, P9a + Fe^{2+}, P9b + Al^{3+}), or a clearly biphasic (fast, then slow) increase in absorbance (*e.g.*, P9b + Fe^{2+}, P10 + Al^{3+}). With ligands having a single binding site (caffeic acid, P9a), the second step (following a second-order step of metal binding) is assumed to reflect a rearrangement in the coordination sphere (possibly involving the phosphate ions) to a more stable complex. With P9b, the two steps could in principle be ascribed to sequential metal binding to the two binding sites. However, as both the UV (Cf) and the visible (Cya) bands are concomitantly intensified (Fig. 3), it is proposed that P9b binds a single Fe^{2+} equivalent simultaneously through its two binding units and that the second (first-order) step most likely reflects a rearrangement in the coordination sphere. This double coordination should occur at a minimal reorganization cost as the two moieties are already in π-stacking interaction within the free pigment.

Similarly, as the free caffeic acid and pigments PA and P9a do not bind Al^{3+} under our conditions, Al^{3+}-P9b binding is probably driven by the joined coordination of Al^{3+} to the cyanidin and caffeoyl moieties stacked onto each other by intramolecular copigmentation. The fast coordination of P10 (2 caffeoyl residues) to Al^{3+} (at least as fast as with the cyanidin derivative P9b) emphasizes the specific affinity of the external caffeoyl residue for Al^{3+}. As the same residue is critical to providing protection against water addition to the peonidin nucleus (Table 1), it can be proposed that the strong π-stacking interactions developed by these two moieties are key to the affinity of P10 for Al^{3+}.

The spectral changes observed in iron - cyanidin binding combine the bathochromic shift featuring the complete conversion of the ligand to the anionic base and the underlying ligand-to-metal charge transfer. As the latter effect is absent with aluminum, the overall bathochromic shift is much weaker (for P9b, 8 nm, *vs*. 36 nm with iron) (Table 2-SI). With Al^{3+}, a small fraction of unbound pigment may also remain in solution (reversible binding). The influence of the acyl residues is critical and, for instance, the iron-induced bathochromic shift drops to 9 nm for nonacylated PA. It is thus proposed that the simultaneous binding of Fe^{2+} by cyanidin and the caffeoyl residue of P9b is the driving force in the intense bluing effect observed with this pigment. By comparison, the highest bathochromic shift achieved by adding Fe^{3+} (1 equiv.) to a neutral solution of red cabbage anthocyanins (non-coordinating HCA residues) is *ca*. 20 nm (8 nm with Al^{3+}) [8].

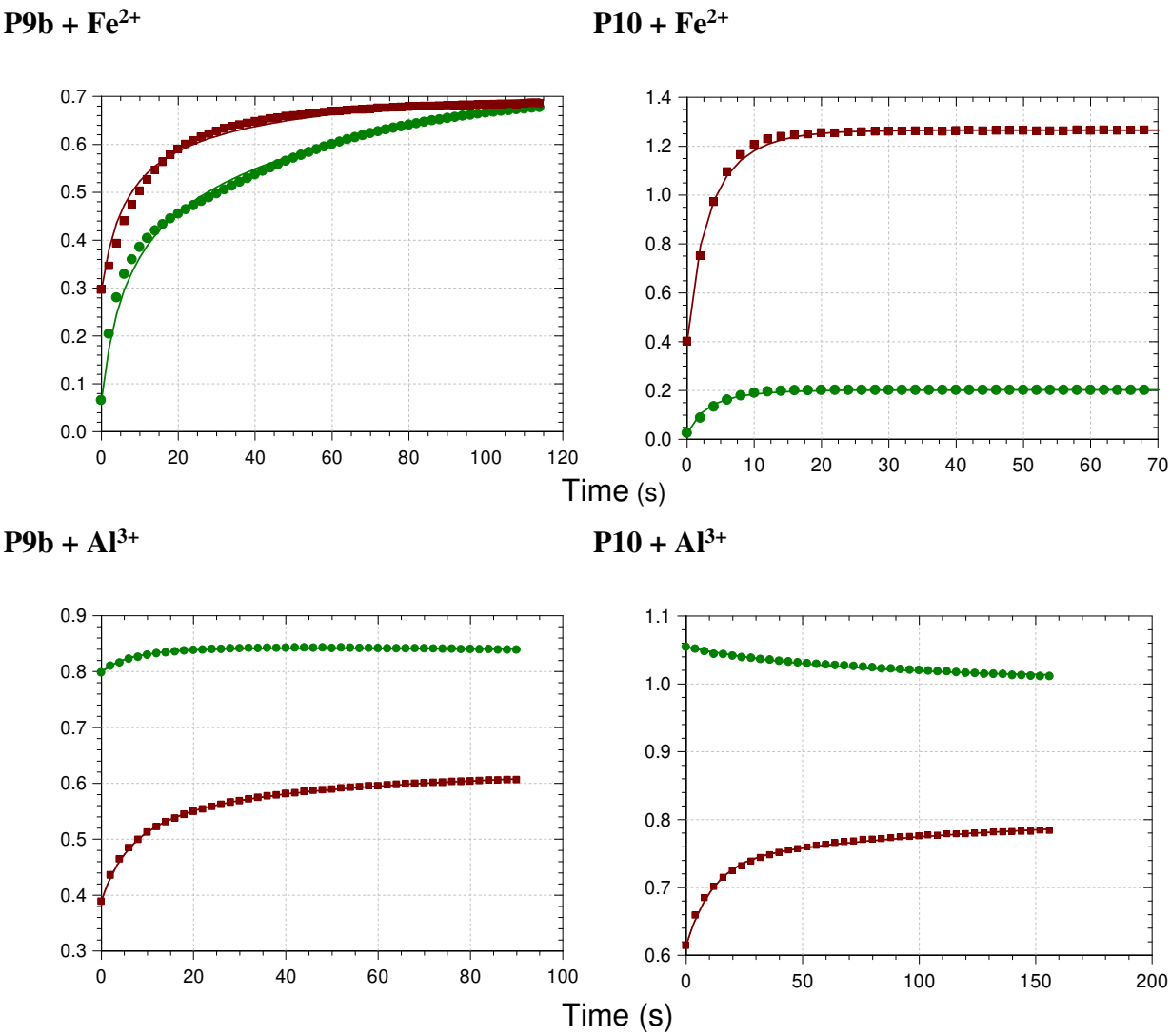

372 **Fig. 3.** The kinetics of metal binding to P9b and P10 (pH 7, 2 equiv. metal ion). ■: Monitoring
373 in the UV range (370 nm), ●: Monitoring in the visible range (Fe^{2+}: 670 nm, Al^{3+}: 550 nm).

374

375 Overall, iron binding appears faster than aluminum binding (when observable), a likely
376 consequence of a stronger competition between phosphate and the anthocyanin's binding sites
377 for Al^{3+}.

378

Table 2. Kinetic analysis of metal – ligand binding (pH 7, 0.01 M phosphate buffer, 25°C).

Metal, Pigment	M equiv.	$10^3\,k_1$ ($M^{-1}\,s^{-1}$) [a]	k_2 (s^{-1}) [b]	λ (nm) [c] $10^3\,\varepsilon_1$ ($M^{-1}\,cm^{-1}$)	λ (nm) [c] $10^3\,\varepsilon_2$ ($M^{-1}\,cm^{-1}$)
Fe, P9a	1	10.6 (± 0.7)	0.17 (± 0.01)	370: 29.9 (± 0.7) 670: 5.9 (± 0.2)	370: 20.5 (± 0.1) 670: 3.7 (± 0.1)
Fe, P9b	1	2.4 (± 0.1)	-	370: 17.5 (± 0.1)	-
		7.2 (± 0.2)	16.9 (± 0.5) x10^{-3}	670: 10.8 (± 0.1)	670: 18.1 (± 0.1)
[d]		3.5 (± 0.1)	16.9x10^{-3}	370: 16.2 (± 0.1) 670: 13.2 (± 0.2)	370: 17.5 (± 0.1) 670: 18.1 (± 0.1)
Fe, P9b	2	10.0 (± 0.2)	23.8 (± 0.4) x10^{-3}	370: 17.2 (± 0.1) 670: 12.3 (± 0.1)	370: 18.6 (± 0.1) 670: 17.7 (± 0.1)
Fe, P10	1	3.7 (± 0.1)	-	370: 29.6 (± 0.1) 670: 4.8 (± 0.1)	
Fe, P10	2	4.3 (± 0.1)	-	370: 31.6 (± 0.1) 670: 5.1 (± 0.1)	
Fe, Cf	1	13.0 (± 0.5)	39 (± 1) x10^{-3}	370: 4.7 (± 0.1) 670: 0.92 (± 0.01)	370: 1.9 (± 0.1) 670: 0.32 (± 0.01)
Fe, PA	1	5.10 (± 0.6)	199 (± 14) x10^{-3}	670: 26.3 (± 0.22)	670: 5.19 (± 0.05)
Al, P9a	1	No binding			
Al, P9b	1	1.3 (± 0.1)	-	370: 12.6 (± 0.1) 610: 21.4 (± 0.1)	-
Al, P9b	2	1.9 (± 0.1)	19 (± 1) x10^{-3}	370: 13.3 (± 0.1) 550: 20.3 (± 0.1)	370: 14.9 (± 0.1) 550: 20.2 (± 0.1)
Al, P10	1	2.2 (± 0.1)	-	370: 13.7 (± 0.1)	-
Al, Cf	1	No binding			
Al, PA’	1	No binding			

[a] k_1: bimolecular rate constant of metal binding leading to complex 1. [b] k_2: first-order rate constant for the possible evolution of complex 1 to complex 2. [c] ε_1, ε_2: molar absorption coefficients of complex 1 and complex 2 at the specified wavelengths. [d] Final (refined) curve-fitting at both wavelengths. M equiv: metal to pigment molar ratio.

3.3. Thermal stability

3.3.1. Rate of degradation

The stability of individual anthocyanins was investigated at pH 7, 50°C (Fig. 4). In the peonidin series, P10 (Peo-Cf,Cf) is more resistant to color loss than PA', a protection afforded by the acyl - peonidin π-stacking interactions (Fig. 4a). In the presence of caffeic acid (2 equiv.), the rate of color loss for PA' is unchanged, thus suggesting that intermolecular copigmentation is ineffective under such conditions. Unexpectedly, total pigment quantification (after acidification) shows that P10 is much less resistant to true (irreversible) degradation than its nonacylated counterpart PA' (Fig. 4b). P11 and P12, which also display caffeoyl residues, have degradation rates close to that of P10 (Fig. 7-SI). Moreover, the addition of caffeic acid (2 equiv.) also accelerates the degradation of PA' (Fig. 4b). By contrast, the irreversible degradation of the red cabbage anthocyanins (acyl = pC, Fl, Sp) is barely impacted by the acylation pattern [4]. Thus, it seems that the redox active caffeoyl residue [23] favors the oxidative degradation of PSP anthocyanins.

Iron – anthocyanin binding is a major way of producing stable blue colors [8,17]. However, even moderate Fe^{2+} concentrations were shown to accelerate the degradation of red cabbage anthocyanins, specifically the non- and monoacylated ones [4]. Nonacylated PA' from PSP (Peo-3-O-Soph-5-O-Glc) and PA, its homolog from RC (Cya-3-O-Soph-5-O-Glc), undergo degradation at similar rates (Fig. 4b). However, PA is much more destabilized by Fe^{2+} addition than PA' (t_{50} = 2h *vs*. 17h). This is consistent with a degradation initiated by iron binding followed by a two-electron transfer to O_2. On the other hand, Fe^{2+} (1.5 equiv.) has no impact on the rate of P10 degradation (Fig. 7-SI). In this case, tight iron – caffeoyl binding cancels the pro-oxidant effect of Fe^{2+}, as observed with the diacylated anthocyanins of red cabbage [4].

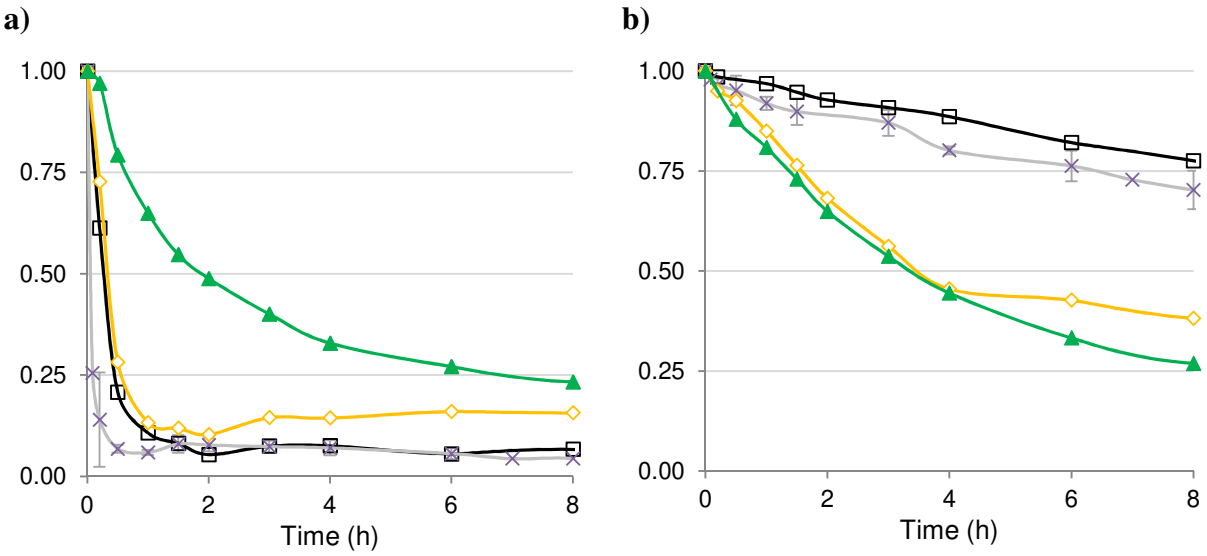

411 **Fig. 4.** Kinetics of **a)** color loss and **b)** pigment degradation (pH 7, 50°C). PA (Cya, no acyl,
412 x), PA' (Peo, no acyl, □), P10 (Peo, Cf, Cf, ▲), PA' + 2 equiv. caffeic acid (◊).

413

414 In summary, caffeic acid, either free or bound to the glycosyl moieties, accelerates the
415 degradation of PSP anthocyanins at pH 7 but this effect can be suppressed by iron - caffeoyl
416 binding. More generally, the presence of redox-active catechols, such as catechins and caffeic
417 acid esters, may contribute to the overall chemical instability of anthocyanin-rich extracts
418 [24]. Indeed, in spite of its higher percentage of diacylated anthocyanins, the PSP extract is
419 less stable than the RC extract at pH 7, 50°C (Fig. 8-SI).

420 *3.3.1. Degradation products*

421 The degradation products of P11 and P12 (diacylated peonidin derivatives having one
422 caffeoyl residue) and of P4 (diacylated cyanidin derivative without caffeoyl residue)
423 supplemented with caffeic acid (1 equiv.) were analyzed by UPLC-MS/DAD. Pigments
424 having lost the caffeoyl residue (*m/z* 905 from P11, *m/z* 961 from P12) were detected as well
425 as diacylsophorose moieties (*m/z* 623 from P11, *m/z* 679 from P12), feruloylsophorose (2.8
426 µM in ferulic acid equiv. after 24h) and caffeoylsophorose (1.3 µM in caffeic acid equiv. after
427 24h) in low concentration. Under similar degradation conditions, *p*-coumaroylsophorose was
428 detected as a major degradation product of red cabbage anthocyanins at pH 7 [3].

429 A group of new pigments also was detected, corresponding to P11 – 2H and P12 – 2H.
430 Similar two-electron oxidized products were not detected with red cabbage anthocyanins
431 under the same conditions [3]. For instance, with P12, 2 isomers of **2** having a *m/z* of 1121

were observed at R_t = 4.0 and 5.2 min (Fig. 5a). Their λ_{max} of 536 nm corresponds to a shift of *ca.* +4 nm compared to P12 (Fig. 9-SI). Products **2** are probably formed by autoxidation of the caffeoyl residue (initiated by metal traces) with concomitant formation of a *o*-quinone and H_2O_2 [18]. The *o*-quinone could then evolve by intramolecular nucleophilic addition of the peonidin nucleus (under its nucleophilic anionic base or hemiketal form), as already observed in an intermolecular version [25,26]. As the *o*-quinone of a caffeoyl residue has several electrophilic centers and the peonidin nucleus (anionic base and/or hemiketal) has 2 nucleophilic centers (C6 and C8), the formation of several isomers is actually possible.

For comparison, a solution of red cabbage anthocyanin P4 (*m/z* 1123) supplemented with caffeic acid was heated under the same conditions. A new pigment noted **1** was detected with a λ_{max} of 525 nm (*vs.* 537 nm for P4) and a *m/z* of 1301 consistent with an oxidative coupling to caffeic acid (Figs 5b & 10-SI). This compound has 3 isomers (R_t = 6.92, 7.16 and 8.30 min) and yields a *m/z* 1141 fragment, corresponding to the P4 hemiketal. Besides, **1** also losses CO_2 to yield a *m/z* 1257 ion. Product **1** is thus proposed to result from the nucleophilic addition of P4 to the caffeic acid *o*-quinone. Similar products have already been observed when nonacylated anthocyanins are treated by the *o*-quinone of caffeic or caffeoyltartaric acid (generated by enzymatic oxidation) [25,26].

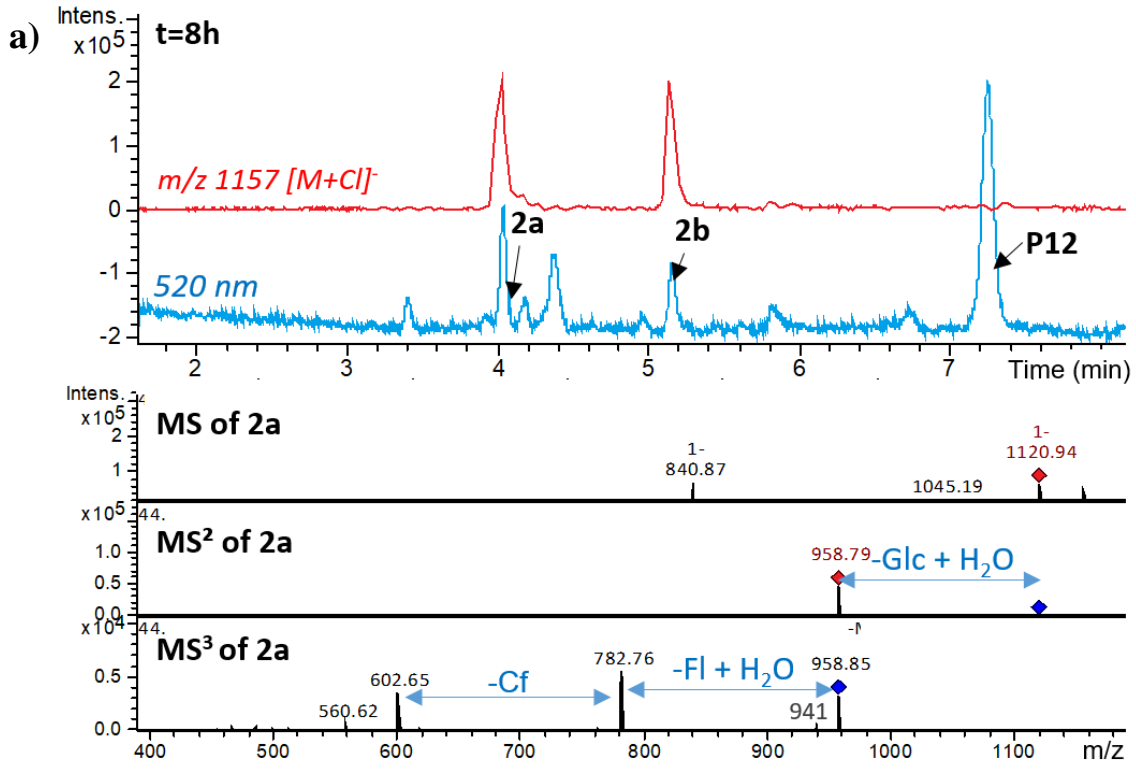

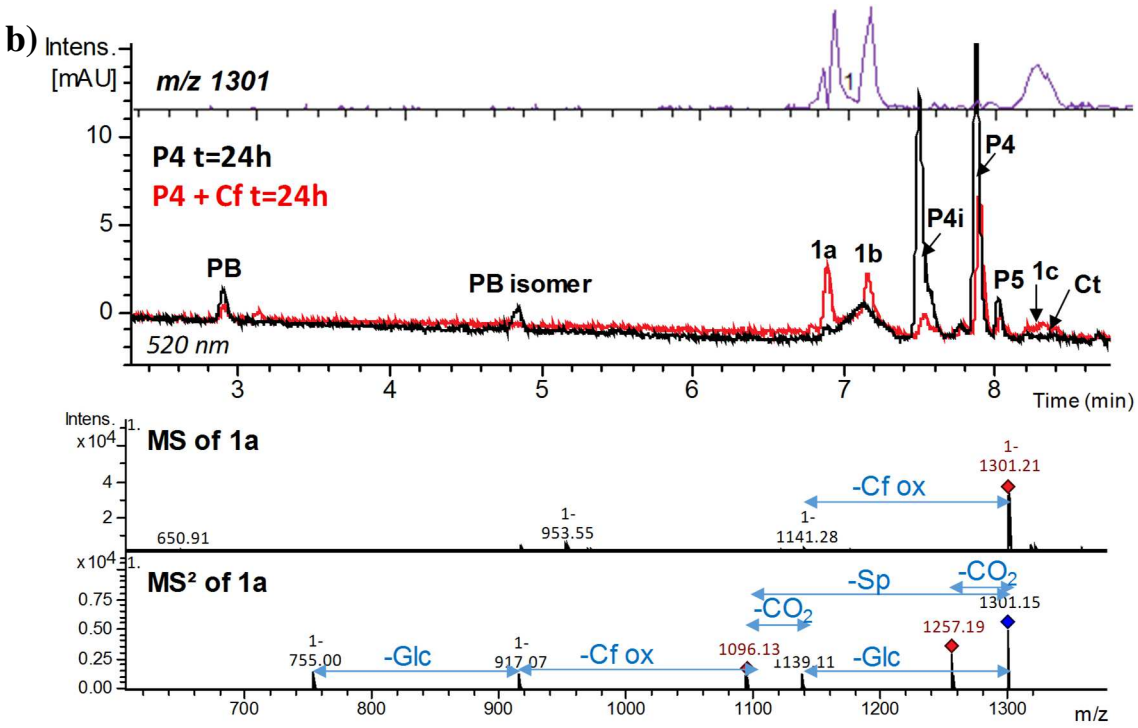

Fig. 5. UPLC-MS/DAD monitoring of thermal degradation at pH 7, 50°C (detection at 520 nm + ion current). **a)** P12 after 8h ($[M-2H]^-$ ion: *m/z* 1123). Detection of two-electron oxidized isomeric pigments 2a and 2b (*m/z* 1121). **b)** P4 after 24h ($[M-2H]^-$ ion: *m/z* 1123). Detection of pigments 1a and 1b (*m/z* 1301) resulting from oxidative coupling between P4 and caffeic acid (1 equiv.). P5: initial contamination. Ct: P4 *trans*-chalcone.

Pigment **1** concentration after 24h at pH 7, 50°C was estimated at 5.2 µM (in cyanin equivalent), *i.e.* roughly equal to the residual P4 concentration (4.9 µM, *i.e.* ca. 10% of the initial concentration). Interestingly, while P4 alone is very prone to isomerization (up to 53%) *via* intramolecular migration of its sinapoyl residue (at C2-OH of Glc-2) [3], addition of caffeic acid inhibits this phenomenon (only 19% under the same conditions).

In brief, acylation by caffeic acid or supplementation by free caffeic acid both concur to making anthocyanins more prone to autoxidation at neutral pH. The anthocyanin derivatives thus formed still absorb in the visible range (Figs 9-SI & 10-SI). Their contribution to the global color and its stability would deserve additional investigation.

4. Conclusion

Diacylated PSP anthocyanins express more intense purple and blue colors in near neutral solution than non- and monoacylated ones. Their color is also more stable, thanks to efficient π-stacking interactions between the acyl residues and the anthocyanidin nucleus. However, a vulnerable point of the PSP anthocyanins evidenced in this work is the presence of redox-active caffeoyl residues that accelerate their oxidative degradation, thus making purple sweet potato extracts less stable than red cabbage extracts, despite the higher content in diacylated anthocyanins of the former. Thus, under moderate heating at pH 7, caffeoyl residues undergo autoxidation to electrophilic/oxidizing *o*-quinones produced by autoxidation of the caffeoyl residues, a reaction probably initiated by iron traces. Metal - caffeoyl binding only weakly modifies the color expressed through a modulation of the acyl - peonidin π-stacking interactions. Through a tight iron coordination, anthocyanins bearing two caffeoyl residues appear resistant to the pro-oxidant effect of moderate Fe^{2+} concentrations (10 to 100 times the trace concentrations in tap water). Al^{3+} binding could be an alternative to erase the redox activity of the caffeoyl residues. On the other hand, a minor PSP pigment combining a cyanidin nucleus and a caffeoyl residue can strongly bind iron through its two interacting catechol nuclei with concomitant strong bathochromism and blue color development.

In summary, diacylated PSP anthocyanins have a high potential for development as natural blue colors, provided that the reactivity of their caffeoyl residues be kept under control. To this purpose, food-grade nucleophiles and antioxidants (thiols, ascorbate) could be worth testing. In crude extracts, a purification step aimed at eliminating caffeoylquinic acids from the PSP extracts could help limit the oxidative degradation of anthocyanins.

Acknowledgements

The authors gratefully thank Dr. Raphaël Plasson (UMR408, Avignon University) for developing the program converting UV-visible spectra into L*a*b* coordinates.

References

[1] Pina F. Chemical applications of anthocyanins and related compounds. A source of bioinspiration. J Agric Food Chem 2014;62:6885−6897. https://doi.org/10.1021/jf404869m.

[2] Dangles O, Fenger J-A. The chemical reactivity of anthocyanins and its consequences in food science and nutrition. Molecules 2018;23:1970. https://doi.org/10.3390/molecules23081970.

[3] Fenger J-A, Robbins RJ, Collins TM, Dangles O. The fate of acylated anthocyanins in mildly heated neutral solution. Dyes Pigments 2020;178:108326. https://doi.org/10.1016/j.dyepig.2020.108326.

[4] Fenger J-A, Moloney M, Robbins RJ, Collins TM, Dangles O. The influence of acylation, metal binding and natural antioxidants on the thermal stability of red cabbage anthocyanins in neutral solution. Food Funct 2019;10:6740–51. https://doi.org/10.1039/C9FO01884K.

[5] Moloney M, Robbins RJ, Collins TM, Kondo T, Yoshida K, Dangles O. Red cabbage anthocyanins: The influence of D-glucose acylation by hydroxycinnamic acids on their structural transformations in acidic to mildly alkaline conditions and on the resulting color. Dyes Pigments 2018;158:342–52. https://doi.org/10.1016/j.dyepig.2018.05.057.

[6] Oliveira H, Basílio N, Pina F, Fernandes I, de Freitas V, Mateus N. Purple-fleshed sweet potato acylated anthocyanins: Equilibrium network and photophysical properties. Food Chem 2019;288:386–94. https://doi.org/10.1016/j.foodchem.2019.02.132.

[7] Trouillas P, Sancho-García JC, De Freitas V, Gierschner J, Otyepka M, Dangles O. Stabilizing and modulating color by copigmentation: Insights from theory and experiment. Chem Rev 2016;116:4937–82. https://doi.org/10.1021/acs.chemrev.5b00507.

[8] Sigurdson GT, Robbins RJ, Collins TM, Giusti MM. Evaluating the role of metal ions in the bathochromic and hyperchromic responses of cyanidin derivatives in acidic and alkaline pH. Food Chem 2016;208:26–34. https://doi.org/10.1016/j.foodchem.2016.03.109.

[9] Sigurdson, GT, Robbins RJ, Collins TM., Giusti MM. Molar absorptivities (ε) and spectral and colorimetric characteristics of purple sweet potato anthocyanins. Food Chem 2019;271:497–504. https://doi.org/10.1016/j.foodchem.2018.07.096.

528 [10] Terahara N, Shimizu T, Kato Y, Nakamura M, Maitani T, Yamaguchi M, et al. Six
529 diacylated anthocyanins from the storage roots of purple sweet potato, Ipomoea batatas.
530 Biosci Biotechnol Biochem 1999;63:1420–4. https://doi.org/10.1271/bbb.63.1420.

531 [11] CIE Standard. Colorimetry — Part 1: CIE standard colorimetric observers | CIE 2004.
532 http://www.cie.co.at/publications/colorimetry-part-1-cie-standard-colorimetric-
533 observers-0.
534 [12] Kim HW, Kim JB, Cho SM, Chung MN, Lee YM, Chu SM, et al. Anthocyanin changes
535 in the Korean purple-fleshed sweet potato, Shinzami, as affected by steaming and
536 baking. Food Chem 2012;130:966–72. https://doi.org/10.1016/j.foodchem.2011.08.031.
537 [13] Xu J, Su X, Lim S, Griffin J, Carey E, Katz B, et al. Characterisation and stability of
538 anthocyanins in purple-fleshed sweet potato P40. Food Chem 2015;186:90–6.
539 https://doi.org/10.1016/j.foodchem.2014.08.123.
540 [14] Silva FAM, Borges F, Guimarães C, Lima JLFC, Matos C, Reis S. Phenolic acids and
541 derivatives: Studies on the relationship among structure, radical scavenging activity,
542 and physicochemical parameters. J Agric Food Chem 2000;48:2122–6.
543 https://doi.org/10.1021/jf9913110.
544 [15] Tomac I, Seruga M. Electrochemical properties of chlorogenic acids and determination
545 of their content in coffee using differential pulse voltammetry. Int J Electrochem Sci
546 2016;11:2854–76. https://doi.org/10.20964/110402854.
547 [16] Mendoza J, Basílio N, Pina F, Kondo T, Yoshida K. Rationalizing the color in heavenly
548 blue anthocyanin. A complete kinetic and thermodynamic study. J Phys Chem B
549 2018;122:4982–92. https://doi.org/10.1021/acs.jpcb.8b01136.
550 [17] Yoshida K, Mori M, Kondo T. Blue flower color development by anthocyanins : from
551 chemical structure to cell physiology. Nat Prod Rep 2009;26:884–915.
552 https://doi.org/10.1039/B800165K.
553 [18] Nkhili E, Loonis M, Mihai S, Hajji HE, Dangles O. Reactivity of food phenols with iron
554 and copper ions: binding, dioxygen activation and oxidation mechanisms. Food Funct
555 2014;5:1186–202. https://doi.org/10.1039/C4FO00007B.
556 [19] Perron NR, Brumaghim JL. A review of the antioxidant mechanisms of polyphenol
557 compounds related to iron binding. Cell Biochem Biophys 2009;53:75–100.
558 https://doi.org/10.1007/s12013-009-9043-x.
559 [20 Moncada MC, Moura S, Melo MJ, Roque A, Lodeiro C, Pina F. Complexation of
560 aluminum(III) by anthocyanins and synthetic flavylium salts: A source for blue and

561 purple color. Inorganica Chim Acta 2003;356:51–61. https://doi.org/10.1016/S0020-
562 1693(03)00394-3.
563 [21] Smyk B, Pliszka B, Drabent R. Interaction between cyanidin 3-glucoside and Cu(II)
564 ions. Food Chem 2008;107:1616–22. https://doi.org/10.1016/j.foodchem.2007.10.037.
565 [22] Mira L, Fernandez MT, Santos M, Rocha R, Florencio MH, Jennings KR. Interactions
566 of flavonoids with iron and copper Ions: A mechanism for their antioxidant activity.
567 Free Radic Res 2002;36:1199–208. https://doi.org/10.1080/1071576021000016463.
568 [23] Hapiot P, Neudeck A, Pinson J, Fulcrand H, Neta P, Rolando C. Oxidation of caffeic
569 acid and related hydroxycinnamic acids. J Electroanal Chem 1996;405:169–76.
570 https://doi.org/10.1016/0022-0728(95)04412-4.
571 [24] Malien-Aubert C, Dangles O, Amiot MJ. Color stability of commercial anthocyanin-
572 based extracts in relation to the phenolic composition. Protective effects by intra- and
573 intermolecular copigmentation. J Agric Food Chem 2001;49:170–6.
574 https://doi.org/10.1021/jf000791o.
575 [25] Kader F, Irmouli M, Nicolas JP, Metche M. Proposed mechanism for the degradation of
576 pelargonidin 3-glucoside by caffeic acid o-quinone. Food Chem 2001;75:139–44.
577 https://doi.org/10.1016/S0308-8146(00)00301-0.
578 [26] Sarni-Manchado P, Cheynier V, Moutounet M. Reactions of polyphenoloxidase
579 generated caftaric acid o-quinone with malvidin 3-O-glucoside. Phytochemistry
580 1997;45:1365–9. https://doi.org/10.1016/S0031-9422(97)00190-8.
581